https://doi.org/10.48048/tis.2025.9217

Enhanced Fluoride Removal from Groundwater Using Napier Grass-Derived Adsorbent: Experimental and DFT Study

Patcharaporn Somkiattiyot[1], Aunnop Wongrueng[1,*], Phacharapol Induvesa[2], Nuttapon Yodsin[3], Sarunnoud Phuphisith[1], Prattakorn Sittisom[1], Pharkphum Rakruam[1], Wiratchon Srisom[1], Patcharaporn Gavila[4], Supoj Chamnanprai[4] and Satoshi Takizawa[5]

[1]Department of Environmental Engineering, Faculty of Engineering, Chiang Mai University, Chiang Mai 50200, Thailand
[2]Department of Environmental Science, Faculty of Science, Silpakorn University, Nakhon Pathom 73000, Thailand
[3]Department of Chemistry, Faculty of Science, Silpakorn University, Nakhon Pathom 73000, Thailand
[4]Intercountry Centre for Oral Health, Department of Health, Ministry of Public Health, Chiang Mai 50000, Thailand
[5]Department of Urban Engineering, Graduate School of Engineering, The University of Tokyo, Tokyo 1138654, Japan

([*]Corresponding author's e-mail: aunnop@eng.cmu.ac.th)

Received: 24 October 2024, Revised: 27 November 2024, Accepted: 4 December 2024, Published: 20 January 2025

Abstract

Lab-scale experiments and Density Functional Theory (DFT) studies were carried out to investigate the efficiency of Napier grass-derived adsorbent (CNP_600) and alkaline modification (CNP_0.2NaOH_600) as low-cost adsorption materials for fluoride removal. CNP that had been treated with an alkaline solution cloud contained more fluoride than the CNP that had been used initially. The NaOH modification of prepared materials promoted a change in surface characteristics that could enhance fluoride removal efficiency. Those adsorbents fitted well with the pseudo-2nd-order kinetic model and declared that the adsorption process was chemisorption. The isotherm study exhibited the best fit with the Langmuir model, resulting in mono-layer adsorption. The experimental adsorption behavior of fluoride ions (F^-) onto CNPs was investigated. The proposed adsorption process involved electrostatic attraction and hydrogen bonding, which were found to be consistent with the results of a Density Functional Theory (DFT) study. The results indicated that the -OH and -COOH groups on the CNPs displayed electron acceptors from the F^- ions. Additionally, the fluoride removal of actual groundwater from the prepared adsorbents was 17 %. The small percentage of adsorption efficiency in groundwater was because of pH and co-exiting ions. Finally, the use of biomass waste as a biochar adsorbent to control the fluoride excess in groundwater in the problematic area could promote the sustainability of water safety for the community, especially in the northern part of Thailand.

Keywords: Adsorption, Fluoride, Fluorosis, Napier grass, Alkaline modification, Biochar, DFT

Introduction

Fluoride (F^-) has beneficial and detrimental effects, depending on its concentration in drinking water. At low concentrations (0.4 - 1.0 mg/L), fluoride is beneficial to the teeth of young children, as it can protect teeth against decay and promote the calcification of dental enamel [1]. On the other hand, the concentration of fluoride in groundwater can cause dental and skeletal fluorosis, bone diseases, mottling of teeth, and lesions of the thyroid, liver and other organs [2]. Fluoride is released into groundwater through the dissolution of fluoride in rocks. Furthermore, fluoride, biotite, topaz, granite, basalt, syenite, and shale are subsurface minerals that can release fluoride into the groundwater [3]. Fluoride contamination in groundwater has been recognized as a serious environmental problem worldwide. Many countries,

such as Tunisia, Morocco, Algeria, and Senegal, encounter excessive fluoride in their drinking water [3]. The World Health Organization (WHO) set the maximum level of fluoride in drinking water as 1.5 mg/L [4]. In addition, the populations in the northern part of Thailand, such as Chiang Mai, Lamphun, and Mae Hong Son provinces, had been exposed to high levels of fluoride from drinking water. Therefore, the standard of fluoride in drinking water in Thailand established by the Ministry of Public Health is 0.7 mg/L. The prevalence of elevated fluoride levels in groundwater within the northern region of Thailand persists as a prominent issue attributed to the local topographical characteristics [5,6]. Extensive research has been undertaken to address the issue of reducing its concentration, both in controlled laboratory settings and on a larger pilot scale [7-9]. However, the general acceptance of such technologies is hindered in numerous regions due to the significant expenses associated with the required equipment and the intricate installation process. Various techniques, including adsorption, ion exchange, precipitation, electrodialysis, and nanofiltration, can be employed as effective strategies to mitigate the high fluoride levels found in groundwater [8-13]. Adsorption is a technique that offers enhanced convenience and potential cost-effectiveness, contingent upon the specific characteristics of the adsorbents employed. Developing nations commonly employ cost-effective adsorbents that are readily accessible within their local regions, often opting for natural adsorbents. Many studies have been published with complex and expensive absorbents; however, in the local area, it is no longer that type of absorbent due to the need for more methodology and the use of many chemicals and procedures [11]. The utilization of agricultural waste or biomass products is also the best practice for applying them as absorbents, which are cheap and have no future complexity for application in the real world. Various types of literature have investigated to use of rice husk, mango (Mangifera indica), and biochar to remove fluoride in water and showed some interesting results in removal efficiency [14]. However, some materials, such as biomass waste found in both raw and modified biochar materials, showed low defluorination at the natural pH and exhibited high removal efficiency at high pH with high-cost modification and a long contact time [15]. To enhance the removal efficiency with chemical and physical modification, the carbonization of biomass materials is the most appropriate option for further applications [16]. Moreover, the adsorption mechanisms were carried out by mean of density functional theory (DFT) to understand our prepared materials for removing the fluoride contaminated in water and groundwater. Density Functional Theory (DFT) is a computational quantum mechanical modeling method widely used to study the electronic structure of atoms, molecules, and condensed matter systems. It plays a crucial role in predicting the physical, chemical, and electronic properties of materials without requiring experimental input, making it an indispensable tool in material and catalyst design. Furthermore, DFT provides insights into reaction mechanisms, adsorption processes, and chemical bonding, allowing a deeper understanding of the adsorption behavior of fluoride ions on the prepared CNP material. In this study, DFT calculations were employed to investigate the adsorption mechanism and to identify which functional groups of the CNP material preferentially interact with fluoride ions. The adsorption behavior of fluoride or other guest molecules on adsorbents is largely influenced by their physical and chemical interactions. Previous studies have highlighted the complexity of pollutant removal processes in water treatment, particularly when using biochar. Various factors, including porous structure, π–π interactions, surface charge, functional groups, and hydrogen bonding, significantly impact adsorption efficiency. For instance, Jawad *et al*. [17] demonstrated that covalent forces arising from electron sharing between pollutants and adsorbents regulate the rate of chemical adsorption. Similarly, Shao *et al.* [18] reported that the primary mechanisms for the adsorption of cationic dyes involve complexation and electrostatic interactions between oxygen-containing functional groups on chemically modified adsorbents and dye molecules.

Therefore, the current research work aims to investigate the carbonization of Napier grass modified with an alkaline condition for fluoride removal from water and to examine adsorption mechanisms, including adsorption kinetics and adsorption isotherms in batches and actual groundwater. Also, the material characterization of prepared materials, including XRD, SEM-EDS, surface charge, porosity, and surface charge

(BET), was examined. Additionally, density functional theory (DFT) was employed to investigate the potential fluoride removal mechanisms, detailing the interactions and primary functional groups between CNP and fluoride ions.

Materials and methods

Synthetic water and actual groundwater

Synthetic water containing 10.0 mg/L of fluoride was prepared from sodium fluoride (NaF) in deionized water. In addition, actual groundwater was collected from Banbuakkhang School. It is located in San Kamphaeng District, Chiang Mai, Thailand. The fluoride concentration in this groundwater was approximately 10.0 mg/L. The colorimetric approach was used to quantify the fluoride concentration in water samples at a wavelength of 570 nm. (Jenway 6400 Spectrophotometer, Jenway, UK).

Material preparation

Napier grass was collected from a cow farm at the Energy Research and Development Institute-Nakornping (ERDI), Chiang Mai University. It was soaked with deionized water following sun drying. Then, it was chopped into a size of 1-3 cm. The prepared Napier grass was separated into 2 Types, including Napier grass cleaned and soaked with deionized water, known as CNP_600, and modified by soaked in 0.2 M of sodium hydroxide (NaOH) and stirred for 2 h at 80 °C, known as CNP_0.2NaOH_600. After that, both types of Napier grass were pyrolyzed at 600 °C for 2 h. Subsequently, they were cooled down, grinded, and sieved in the size range of 60 - 100 mesh. CNP_600 and CNP_0.2NaOH_600 adsorbents were completely washed and soaked with deionized water. Finally, both adsorbents were dried in the oven and transferred to a desiccator.

Materials characterization

The physical and chemical properties of materials were analyzed. The surface morphologies and micro chemical compositions of CNP_600 and CNP_0.2NaOH_600 adsorbents were examined using an SEM/EDS (JSM-IT300). The crystalline structure of CNP_600 and CNP_0.2NaOH were confirmed via X-ray diffraction (XRD) patterns using a Bruker/D8ADVANCE, Germany. The porosity and surface area (BET) were measured by nitrogen adsorption isotherm using Autosorb 1 MP, Quanta Chrome Instrument, USA. The surface function groups of materials were analyzed using a Fourier transform spectrophotometer over a range of 400 to 4,000 cm^{-1} with a resolution of 4 cm^{-1} (PerkinElmer). The points of zero charge (pH_{pzc}) of CNP_600 and CNP_0.2NaOH_600 adsorbents were adapted and determined. After weighing 0.1 g of the CNP_600 and CNP_0.2NaOH_600 adsorbents, they were added to 100 mL of deionized water with a pH range of 3.0 to 12.0 that had been adjusted with sodium hydroxide or nitric acid. The combined samples were then agitated for 24 h at 200 rpm using a shaker (GFL, Orbital Shaker 3017, Germany). The final pH of every sample was then determined. Plotting the initial and final pH values allowed for the identification of the pHpzc. The common peak of the plot of the relationship between the initial and final pH solutions was used to examine the adsorbent's point of zero charge (PZC).

Adsorption experiment

In the batch adsorption studies, synthetic water with a fluoride content of 10.0 mg/L was utilized. 0.5 g and 1.0 g of the adsorbents were mixed into 100 mL of synthetic water at pH 7.0, respectively, for the adsorption kinetics and isotherm studies (controlled by a phosphate buffer). A rotary shaker (GFL, shaker 3017) was used to combine these samples at room temperature at 200 rpm. The CNP_600 and CNP_0.2NaOH_600 adsorbents were extracted from the solution using a nylon syringe filter (nominal pore size 0.22 µm, Chrom Tech) after the mixing was stopped at various adsorption durations ranging from 0 to 48 h. The filtrates were analyzed for residual fluoride concentrations. The adsorption isotherms were studied by varying the initial fluoride concentrations from 1 mg/L to 100 mg/L. The pH of the solution was controlled by phosphate buffer at 7.0. The equilibrium time was based on the kinetics study results (6 h). After adsorption at equilibrium time, the solution was filtrated and measurement residue fluoride as described in the kinetic study. In addition, the adsorption of actual groundwater was obtained from the excess fluoride contamination with an initial concentration of 10 mg/L of fluoride, and the adsorption

mechanism was similar to that of synthetic fluoride water.

Adsorption mechanism

Adsorption kinetics

The kinetics of fluoride adsorption were determined using 2 alternative kinetic models, which included pseudo-1st-order and pseudo-2nd -order equations. The equation of pseudo-1st-order and pseudo-2nd-order models is given by Eqs. (1) - (3), respectively.

The pseudo-1st-order equation is presented as follows:

$$\ln\left(\frac{q_e}{q_e-q_t}\right) = k_{\mathrm{p1}}t \quad (1)$$

Which can be rearranged in linear form as follows:

$$\log(q_e - q_t) = \log(q_e) - \frac{k_{p1}t}{2.303} \quad (2)$$

where q_t is the adsorption capacity at time t (mg/g), q_e is the adsorption capacity at equilibrium (mg/g), t is time (min), and k_{p1} is the pseudo-1st-order rate constant (min^{-1}).

The pseudo-2nd-order equation is applied as follows.

$$\frac{t}{q_t} = \frac{1}{\mathrm{k_{p2}}q_e^2} + \frac{t}{q_e} \quad (3)$$

where q_t is the adsorption capacity at time t (mg/g), q_e is the adsorption capacity at equilibrium (mg/g), t is time (min), and k_{p2} is the pseudo-2nd-order rate constant (g/mg·min).

Adsorption isotherms

Three isotherm models (linear, Langmuir, and Freundlich) were used to investigate the adsorption behavior of fluoride on CNP_600 and CNP_0.2NaOH_600 adsorbents.

The linear model equation is shown in Eq. (4)

$$q_e = K_p C_e \quad (4)$$

where K_p is the linear partition and C_e is the concentration at the equilibrium of fluoride.

The Langmuir isotherm is as follows:

$$q_e = \frac{q_0 K_F C_e}{1+K_F C_e} \quad (5)$$

Which can be rearranged in the linear form as follows:

$$\frac{1}{q_e} = \frac{1}{K_F q_0}\frac{1}{C_e} + \frac{1}{q_0} \quad (6)$$

where q_0 is the amount of fluoride adsorbed per unit weight of adsorbent (mg/g), q_e is the total amount of fluoride adsorbed at equilibrium (mg/g), Ce is the concentration of the fluoride in the solution at equilibrium (mg/L), and K_F is the constant related to the energy of sorption (L/mg).

The Freundlich isotherm is shown by the following equation:

$$q_e = K_F C_e^{1/n} \quad (7)$$

Which can be rearranged in the linear form as follows:

$$log q_e = \frac{1}{n} log C_e + log K_F \quad (8)$$

where q_e is the total amount of fluoride adsorbed per unit weight of adsorbent at equilibrium (mg/g), C_e is the concentration of the fluoride in the solution at equilibrium (mg/L), K_F is the Freundlich constant (L/g), and n is the Freundlich constant (dimensionless).

Computational method

The optimizations were performed using the density functional theory (DFT) along with Becker's 3-parameter gradient-corrected exchange potential, combined with the Lee−Yang−Parr gradient-corrected correlation potential (B3LYP)[1–3] and including Grimme's D3 dispersion correction (B3LYP-D3)[4] and the 6-31G++(d,p) People basis set to adequately describe the Van der Waals interactions and give proper geometries of molecular clusters. The simulation was carried out in a vacuum environment since the effects of

water revealed that the findings obtained using the conductor-like polarizable continuum solvent model (C-PCM) differed only slightly qualitatively. All calculations were conducted using the Gaussian 16 software package. The adsorption energy (E_{ads}) quantifies the stability of the CNP and fluoride ion (F^-) is calculated as the difference between the energy of the complex ($E_{F\text{-}CNP}$) and the sum of the energies of the isolated CNP adsorbate (E_{CNP}) and the fluoride ion molecule (E_F) in their fully relaxed gas-phase geometries as the following Eq. (9) [19-22].

$$E_{ads} = E_{F-CNP} - E_{CNP} - E_F \quad (9)$$

Results and discussion

Physio-chemical properties of materials text

The physical properties of CNP_600 and CNP_0.2NaOH_600 adsorbents were investigated and illustrated in **Figure 1**. CNP_600 and CNP_0.2NaOH_600 adsorbents exhibited a smooth surface. Although CNP_600 and CNP_0.2NaOH_600 adsorbents showed a smooth surface, an irregular shape of CNP_0.2NaOH_600 was observed after NaOH modification. Based on SEM images, the CNP_0.2NaOH_600 exhibited surface smoothness after treatment with NaOH, resulting in an increase in internal spaces and enhancing an active site [23]. This could lead to the absorption of fluoride into the physicochemical characteristics and an improvement in the fluoride's adsorption capacity. In addition, NaOH treatment introduces hydroxyl (-OH) groups onto the surface of Napier grass biochar. These groups can increase the biochar's hydrophilicity and enhance its interaction with water molecules and contaminants [24].

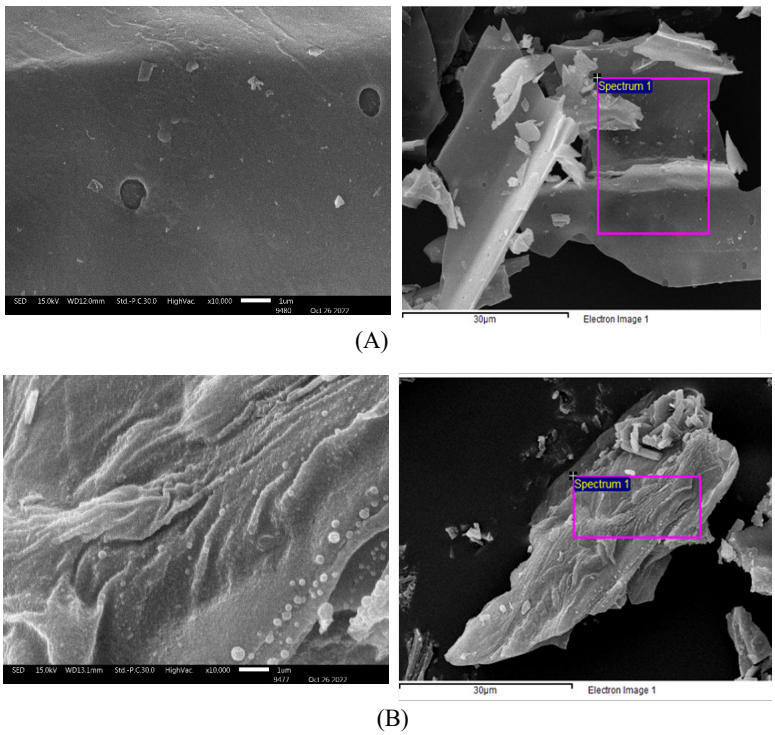

Figure 1 SEM-EDS analysis of (A) CNP_600 and (B) CNP_0.2NaOH_600.

The quantitative chemical composition of CNP_600 and CNP_0.2NaOH_600 adsorbents was analyzed using an energy-dispersive X-ray microanalyzer (SEM-EDS). The chemical composition of CNP_600 and CNP_0.2NaOH_600 adsorbents exhibited different types of elements, as shown in **Table 1**. The highest proportion of CNP_600 was C followed by O and K, respectively. In addition, the CNP_0.2NaOH_600 (wash with NaOH) showed a similar trend to CNP_600. The carbon content of both prepared materials increased when compared to the original Napier grass (45.10 % wt.) [30]. The increase

of carbon contents in CNP_600 and CNP_0.2NaOH_600 can be related to the carbonization process, which involves a restructuring of the carbonaceous structure by breaking less stable chemical bonds in Napier grass [31]. Furthermore, the contents of O, Na, and K were notably elevated in the NaOH-modified materials, particularly the Na element, which was from 0%wt to 1.8%wt. This confirms the successful grafting of NaOH**.**

To investigate the functional groups of CNP_600 and CNP_0.2NaOH_600 surfaces, the FTIR spectra were performed using FTIR. The CNP_600 and CNP_0.2NaOH_600 were packaged as dispersions of a K_{Br} pellet. The IR spectra are shown in **Figure 2**. The minor peaks at 871 and 873 cm^{-1} are exhibited in confirmed calcite biochar materials in both materials [25]. The IR results exhibited similar trends with other research, including peaks at 1,099 and 1,038 cm^{-1} showed C-O and C-O-C stretching, and peaks at 1561 and 1565 cm^{-1} which were assigned to C=C stretching of CNP_600 and CNP_0.2NaOH_600, respectively. The shift of C-O and C-O-C stretching is due to NaOH modification. The board peaks of -OH groups were observed at a range of 2,400 - 3,500 cm^{-1} [26].

Table 1 Elemental analysis of CNPs by EDS mapping.

Materials	Weight %				Atomic %			
	C	O	Na	K	C	O	Na	K
CNP_600	90.6	8.3	0.0	1.1	93.2	6.4	0.0	0.4
CNP_0.2NaOH_600	79.4	14.4	1.8	2.0	85.6	11.6	1.0	0.6

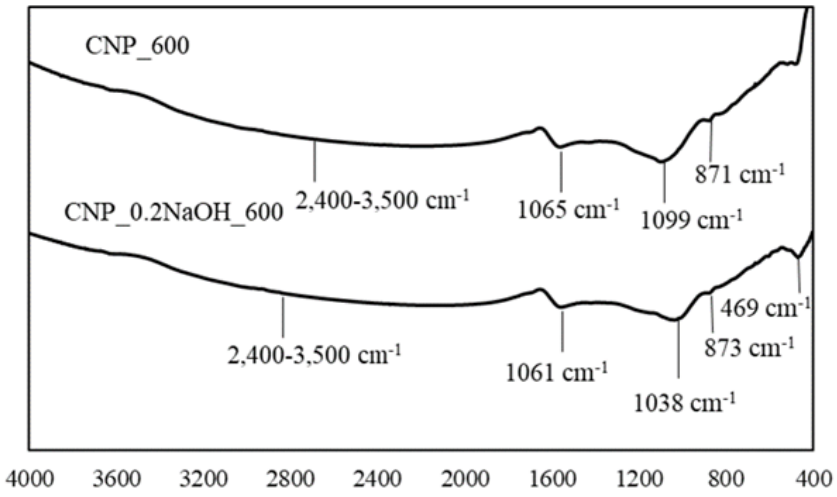

Figure 2 FTIR spectra of CNP_600 and CNP_0.2NaOH_600.

The XRD patterns of the CNP_600 and CNP_0.2NaOH_600 are shown in **Figure 3**. The intensity of the diffraction patterns was expressed in terms of Bragg's angle (2θ). The broad peaks were detected at a 2θ value at around 20 - 62 ° and 22 - 32 ° respectively, these regions indicate elements with an amorphous structure. The Napier grass-derived adsorbents were mostly amorphous in nature, but they possessed a few crystalline structures [27]. The amorphous structure of a biomass is determined by the hemicellulose and lignin [28]. Their adsorption applications benefit from this desired feature [29]. Sharp peaks were observed at 2θ values 22.33, 25.8, 29.4 and 32.3 ° respectively, corresponded to crystalline cellulose, and the intensity of these peaks increased with increasing NaOH concentration. The results were consistent with the elemental analysis, which indicates that the elements are formed at the surface of the adsorbent.

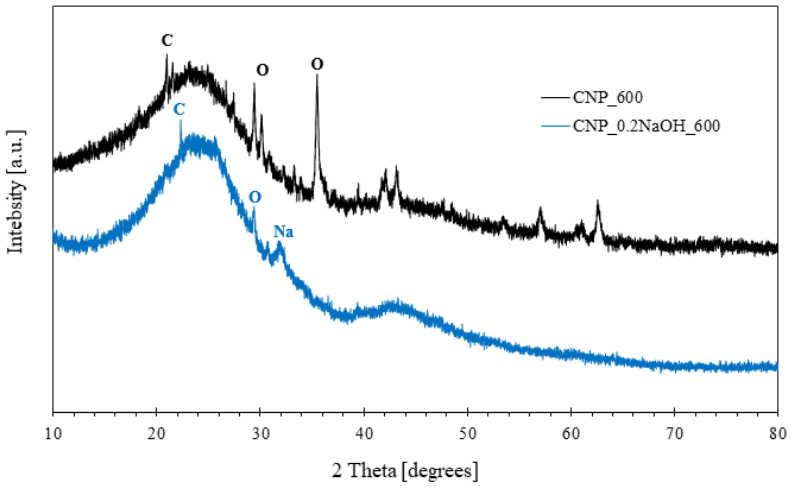

Figure 3 X-ray Diffraction pattern of CNP_600 and CNP_0.2NaOH_600.

The porosity and surface area of CNPs were investigated by nitrogen adsorption isotherm using BET and BJH methods, respectively. (**Figure 4** and **Table 2**). The calculated BET surface area of CNP_600 (washed with deionized water) and CNP_0.2NaOH_600 (washed with base) adsorbents were 182.5 and 115.1 m^2/g, respectively. The pore volume of CNP_600 and CNP_0.2NaOH_600 adsorbents were 0.066 and 0.036 cc/g, respectively. The reduction in the pore volumes of CNP_0.2NaOH_600 indicated control of NaOH on the CNP surface. Moreover, the hysteresis loop of both CNP_600 and CNP_0.2NaOH_600 adsorbents represented the mesopore adsorbents.

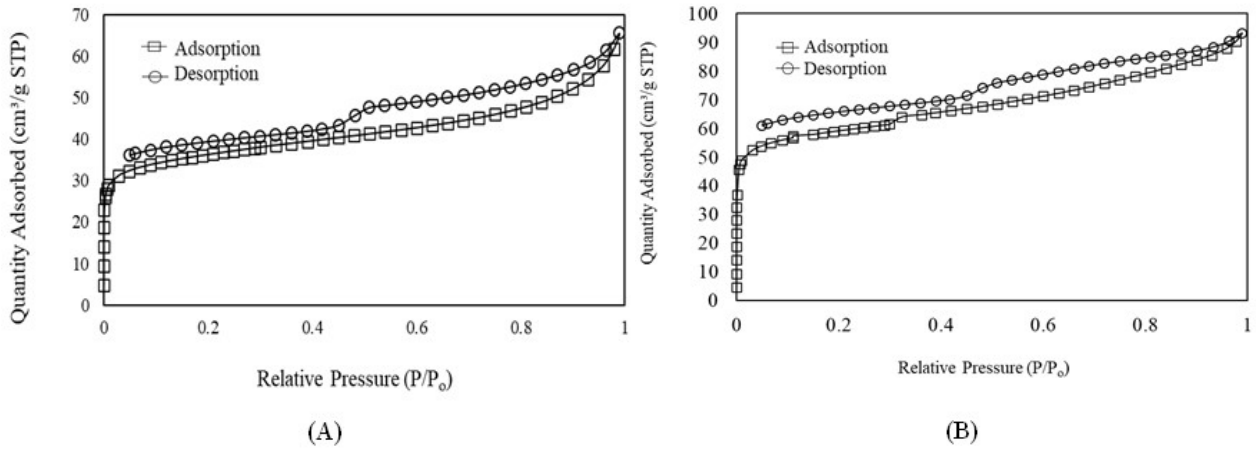

Figure 4 Nitrogen adsorption isotherm (BET) results (A) CNP_600 and (B) CNP_0.2NaOH_600.

Table 2 BET characterization results of the CNP_600 and CNP_0.2NaOH_600.

Materials	CNP_600	CNP_0.2NaOH_600
Specific surface area (m^2/g)	182.5	0.066
Micropore volume (cm^3/g)	115.1	0.036

The point of zero charges (PZC) of CNP_600 and CNP_0.2NaOH_600 adsorbents was investigated by considering the common plateau of the plot of the relationship between the initial pH solution and final pH solution after 24 h. The point of 0 charge (pH_{pzc}) of CNP_600 and CNP_0.2NaOH_600 adsorbents were

approximately 8.0 and 10.0, respectively, as shown in NaOH treatment typically increases the pH of the PZC towards higher values. This shift occurs because the hydroxyl groups contribute to the surface becoming more negatively charged. As a result, the biochar may exhibit a higher PZC compared to untreated biochar

Figure 5. CNP_0.2NaOH_600 displays a pH_{pzc} value of 10, indicating that its surfaces exhibit positive charges of prepared materials when the pH of the solution (approximately 7.0) is lower than the pH_{pzc} and will promote the electrostatic attraction conducive to high adsorption of F^- ions [32,33].

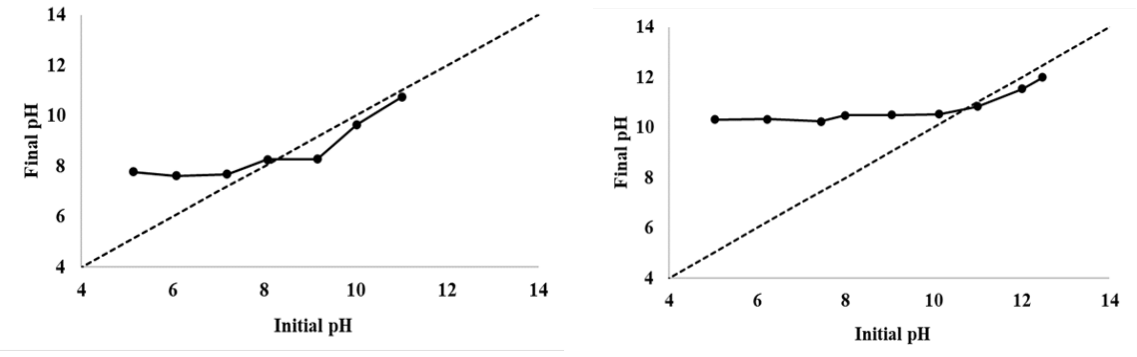

(A) (B)

Figure 5 pH_{pzc} results (A) CNP_600 and (B) CNP_0.2NaOH_600.

Consequently, the hydrated F^- ions can be easily adsorbed onto the positively charged sites than CNP_600, whose pH is slightly equal to pH_{pzc}. When the pH is equivalent to the point of zero charge (PZC), the surface charges of an adsorbent are either neutral or close to 0. This suggests that the surface charge of prepared materials is mostly influenced by the interaction between the material's surface and the ions present in the solution. Understanding the PZC is crucial for fluoride removal and other adsorption applications. Below the PZC, the biochar surface tends to be positively charged, favoring the adsorption of anions like fluoride through electrostatic attraction. Above the PZC, the surface becomes negatively charged, influencing the adsorption behavior towards cations or affecting interactions with different contaminants [32].

Adsorption kinetics, isotherms, and mechanism

The adsorption kinetic of fluoride adsorption on CNP_600 and CNP_0.2NaOH_600 adsorbents are illustrated in **Figure 6**. CNP_600 and CNP_0.2NaOH_600 adsorbents rapidly adsorbed fluoride in the 1st hour. After 1 h, the fluoride adsorption regularly slowed until it reached equilibrium at 6 h. The highest adsorption fluoride capacity on CNP_600 adsorbents at equilibrium was 0.0530 mg/g and CNP_0.2NaOH_600 was 0.1946 mg/g, respectively.

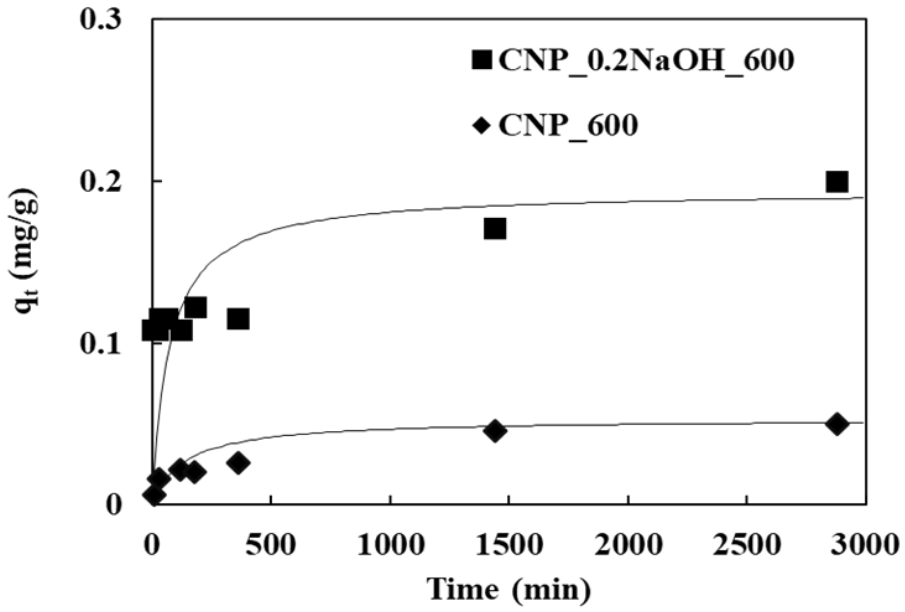

Figure 6 Adsorption kinetics study of CNP_600 and CNP_0.2NaOH_600.

The rate of defluorination was quantitatively ascertained using 2 distinct kinetic models, including pseudo-1st order and pseudo-2nd-order equations. **Table 3** provides a summary of all adsorption kinetic model computations. The kinetic data of CNP_600 and CNP_0.2NaOH_600 adsorbents represented a good correlation (R^2) with the pseudo-2nd-order model (R^2 = 0.9964 and 0.9979, respectively). The results indicated a chemisorption process between absorbent and adsorbate, especially in the presence of surface modification with an alkaline solution [34].

Table 3 Kinetic parameter of fluoride adsorption.

Materials	Pseudo 1st order			Pseudo 2nd order			
	k_1 (min^{-1})	q_{e1} (mg/g)	R^2	k_2 (g/mg*min)	q_{e2} (mg/g)	h	R^2
CNP_600	–0.0007	0.2306	0.7610	0.1455	0.0530	0.0004	0.9964
CNP_0.2NaOH_600	–0.0001	0.2945	0.1977	0.0684	0.1946	0.0026	0.9979

When considering the k_2 parameter from the pseudo-2nd-order model, the rate of CNP_600 was higher than that of CNP_0.2NaOH_600 because of the flat surface resulting in increased speed of fluoride adsorption [35]. According to the results of the kinetic model, chemisorption is responsible for the removal of fluoride by CNP_0.2NaOH_600 and is mostly attributed to the bonding interactions between fluoride ions and hydroxyl groups present in the adsorbent material [36,37]. Chemical interactions occur between the functional groups present on the surface of the carbon-based material (CNP_0.2NaOH_600) and fluoride ions. Functional groups that contain oxygen, such as hydroxyl (OH), carboxyl (COOH), and carbonyl (C=O) groups, could engage in hydrogen bonding with fluoride ions.

The formation of these chemical bonds leads to enhanced and more selective adhesion between the adsorbent and fluoride.

The process of comparing the adsorption isotherm of fluoride with CNP_600 and CNP_0.2NaOH_600, which is the carbonization of biomass waste, entails the investigation of the interaction between various forms of prepared adsorbents and fluoride ions present in a solution. The adsorption isotherm serves as a crucial instrument for investigating the behavior of adsorption, providing insights into the quantity of adsorbate that is

adsorbed onto an adsorbent at different concentrations under conditions of equilibrium.

The isotherm models that are frequently employed in scientific research encompass the Langmuir and Freundlich isotherms. The adsorption isotherm results of linear, Langmuir, and Freundlich models are shown in **Figure 7** and **Table 4**, respectively.

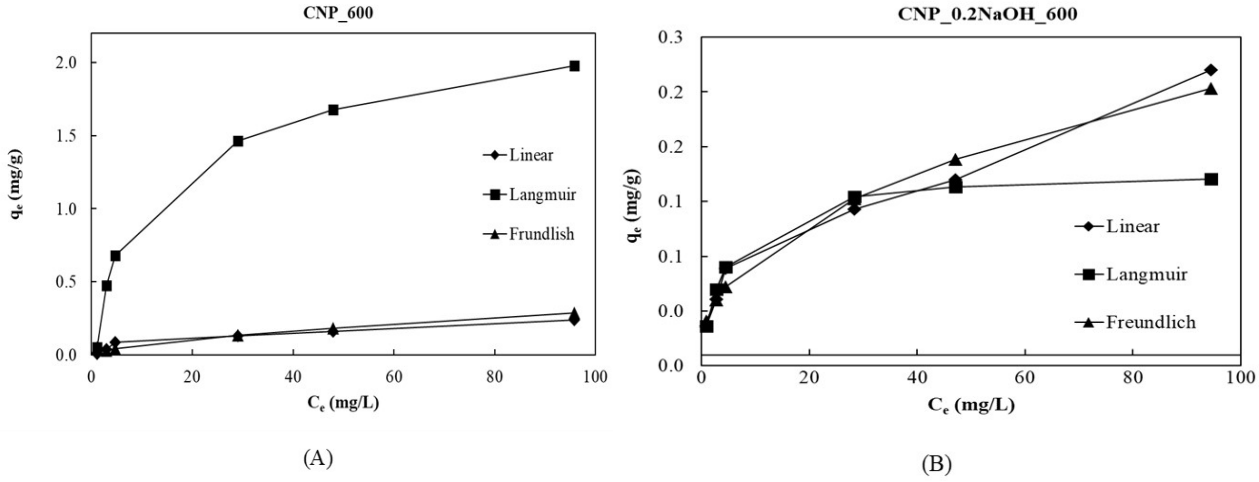

Figure 7 Adsorption isotherm study (A) CNP_600 and (B) CNP_0.2NaOH_600.

Besides, the isotherm parameters of the fluoride absorption on the Napier grass-derived adsorbents (CNP_600 and CNP_0.2NaOH_600) affect fluoride removal. Adsorption studies of fluoride on CNP_600 and CNP_0.2NaOH_600 plots of all obtained isotherm data R^2 of Linear 0.9009 and 0.9176, R^2 of Langmuir 0.9393 and 0.9801 and R^2 of Freundlich 0.8426 and 0.9720 exhibited a linear function of fluoride adsorption. The best R^2 values were represented by the Langmuir model of CNP_0.2NaOH_600. It was indicated that homogenous adsorption was exhibited on the adsorbent surface by monolayers of adsorption [7].

Table 4 Fluoride adsorption (biochar adsorbents) based on Langmuir model.

Materials (biochar)	Adsorption capacity (mg/g)	Ref.
CNP_600	0.17 (25 °C)	This study
CNP_0.2NaOH_600	0.20 (25 °C)	This study
Pinewood	7.66 (25 °C)	[33]
Pine bark	9.77 (25 °C)	
Coffee ground	0.22 (35 °C)	[34]
Rice husk ash	2.91 (25 °C)	[35]

These results could be confirmed with SEM images of materials surface that exhibit the flat and smooth surface. It is indicated that the Langmuir isotherm offers valuable insights into the process of monolayer adsorption, operating on the assumption of a homogeneous adsorption surface that possesses a certain number of identical adsorption sites [41]. Compared with other biochar materials, the isotherm results showed a similar model to the Langmuir isotherm model as shown in **Table 5**. Even though the adsorption capacity is lower using agricultural waste as adsorption materials by easy production (pyrolysis) could be practically set to exceed the F^-contamination area.

Table 5 Isotherm parameters of fluoride adsorption.

Model	Parameters							
	Linear		Langmuir			Freundlich		
	R^2	K_p, L/g	R^2	q_m, mg/g	K_L, L/g	R^2	1/n	K_F, L/g
CNP_600	0.9009	0.0022	0.9393	–0.2562	–0.0288	0.8426	0.6480	0.0150
CNP_0.2NaOH_600	0.9176	0.0030	0.9801	0.1691	0.2045	0.9720	0.4442	0.0323

In summary, the adsorption mechanism depends on the characteristics of both the adsorbent material and the fluoride ions in the solution, as previously mentioned. The adsorption process is subject to the effects of multiple parameters, including the surface physio-chemical properties of the adsorbent, the concentration of fluoride ions, pH levels, temperature, and the duration of contact. Hence, the adsorption process of CNP_0.2NaOH_600 for the removal of fluoride adheres to the Langmuir isotherm model, exhibiting a pseudo-2nd-order fit. The generation of a monolayer shows that the fluoride adsorption process on CNP_0.2NaOH_600 is primarily due to chemisorption, as verified by the previously stated adsorption isotherm and kinetics studies. Based on CNPs functional groups, the sorption mechanism responsible for the removal of fluoride by CNP_0.2NaOH_600 is mostly attributed to the electrostatic and H-bonding processes involving fluoride ions and hydroxyl groups present within the adsorbent materials similar to those presented with previously studied [36]. Therefore, the primary mechanisms involved in fluoride removal by NaOH-functionalized biochar include surface adsorption, H-bonding, and possibly electrostatic attraction, and surface adsorption involves the physical binding of fluoride ions to active sites on the biochar surface [38,42].

DFT calculation

To understand the adsorption behavior of fluoride ions on prepared CNP material, DFT calculations were used to investigate the adsorption mechanism. Initially, the optimized CNP surface is shown in **Figure 8**.

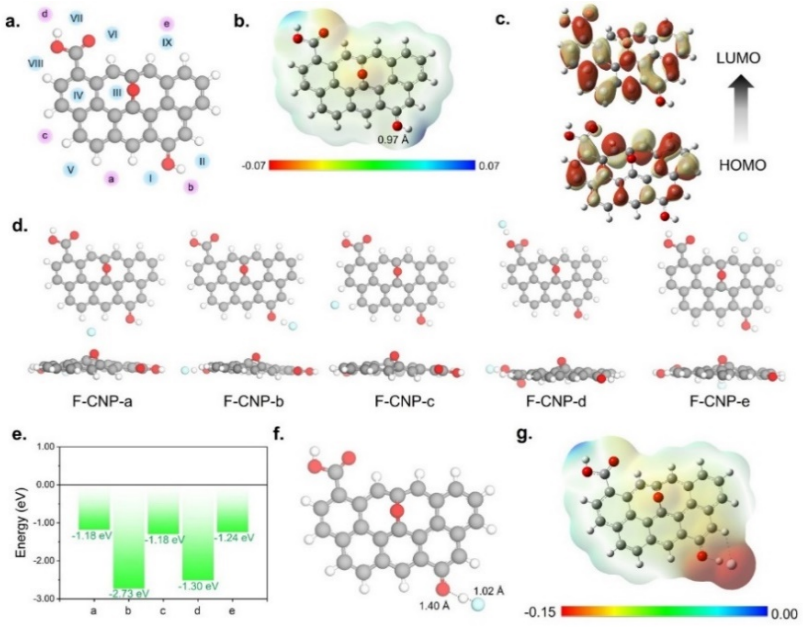

Figure 8 (a) Optimized structure of CNP with all possible F^- adsorption (blue) and all stable F^- adsorption (pink). (b.) ESP of CNP and interaction mechanism of CNP with F^- based on (c.) HOMO-LUMO, and (d.) all stable configurations of interactions between CNP and F^-. (e.) Adsorption energy of all stable configurations. (f.) the most stable configuration between CNP and F^- and (g.) MEP. (gray, white, blue, and red balls denoted C, H, F, and O atoms, respectively).

Based on the experimental results, we have modeled the CNP surface with the -COOH, -CO and -O- functional groups, which correspond well with the IR spectrum. To further analyze molecular interaction sites, we examined electrostatic potential maps (EPS), which measure the strength of nearby charges, nuclei, and electrons at specific positions. ESP enables the visual identification of a molecule's charge distribution, revealing Lewis's acid and Lew's base sites. Our calculations indicated that the O atoms in the functional groups (-COOH, -OH, and -O-) are negatively charged (represented in red), suggesting these regions could donate electrons and be targets for nucleophilic attack. The H atoms on the CNP surface exhibited lower potential (represented in blue), making them targets for electrophilic attack with fluoride ions. ESP analyses showed that the O atoms in the functional groups and other regions of CNP interacted in electrophilic and nucleophilic manners, respectively. The interaction mechanisms were investigated by determining the highest occupied molecular orbital (HOMO) and the lowest unoccupied molecular orbital (LUMO) of CNP using frontier molecular orbital theory (**Figure 8(c)**), which indicated the active sites' ability to accept or donate electrons, thus determining the chemical reaction tendency. Previous studies suggested that the π electron donor-acceptor interaction involves π electrons in both absorbent and adsorbate. (1-3) In contrast, the H atoms in CNP and functional groups like -OH and -COOH acted as electron acceptors from fluoride ions [43].

To offer a more detailed description of the contact strength between fluoride ions and CNP, DFT simulations were used to describe multiple interaction configurations and quantify the adsorption energy (**Figure 8(e)**). We explored all possible fluoride adsorptions (marked as blue sites). After fully optimizing all possible complexes, we identified 5 stable fluoride adsorption sites, including -COOH, -OH, and H atom sites. Interestingly, the -O- site was not found due to its nucleophilic region. The 5 stable structures are shown in **Figure 8(d)**. The adsorption energy (Eads) for all structures was negative for the CNP models, indicating favorable spontaneous adsorption of fluoride ions. A lower adsorption energy suggests more conducive adsorption and the Eads trend showed that H atoms in -COOH and -OH functional groups were the main adsorption sites due to their high electrophilic regions. The most likely interaction between CNP and fluoride ions was found between the -OH in CNP (Configuration b), with a bond distance of 1.20 Å between H and F^-. The shorter bond length demonstrated a stronger interaction force. The adsorption energy of fluoride ion adsorption is calculated to be –2.73 eV. Additionally, the O-H bond lengthened from 0.97 Å to 1.40 Å, confirming the strong interaction between CNP and fluoride ions [44,45].

Fluoride removal from actual groundwater

The initial fluoride concentration in the groundwater was 10.2 mg/L. It was found that the concentration of fluoride was very high, exceeding the quality standard for groundwater used for consumption, with no more than 0.7 mg of fluoride per liter. This groundwater cannot be directly used for drinking and cooking. Fluoride removal of CNP_0.2NaOH_600 and CNP_600 absorbents was approximately lower than 20 %. The pH of the sample of water used in the present study was determined to be 8.0 and when compared to CNP_0.2NaOH_600 and CNP_600 absorbents, the base-modified CNP_0.2NaOH_600 exhibited a higher removal efficiency due to its positive surface charge (pH < pHpzc), indicating its strong adsorption capacity [7]. However, the low adsorption capacity of both carbon materials may be due to the pH of the groundwater solution (pH = 8.0) used in this study. Previous studies indicated that the removal of fluoride by these materials is more effective in acidic groundwater (pH less than 3) [46,47]. In addition, actual groundwater contains other co-ions that can compete with fluoride ions during adsorption onto material surfaces as a consequence of the effect of adsorption capacity and There is a possibility that fluoride ions and co-existing anions in the aqueous solution will compete for adsorption sites during the defluorination process, which will have a detrimental impact on the capacity of the defluorination process [48]. Although the removal efficiency of prepared materials is low, Napier grass biochar is a sustainable and low-cost adsorbent, especially when compared to conventional methods like activated carbon. The NaOH functionalization process is relatively simple and can be conducted using inexpensive reagents, making it economically viable for large-scale applications and promoting sustainable resource management.

Conclusions

Based on this study, the optimum conditions for original Napier grass-derived and activating it with sodium hydroxide (NaOH) were examined for fluoride removal in synthetic and actual groundwater. The results found that the Napier grass-derived adsorbent was activated with concentrated sodium hydroxide (NaOH) 0.2 molar under the pyrolysis process at 600 °C (CNP_600 and CNP_0.2NaOH_600) for 120 min and the specific surface areas of those adsorbents were 182.5 and 115.1 m^2/g of CNP_600 and CNP_0.2NaOH_600, respectively. The pore volumes of those adsorbents were 0.066 cm^3/g and 0.036 cm^3/g of CNP_600 and CNP_0.2NaOH_600, respectively. In addition, the point of zero charges of CNP_600 and CNP_0.2NaOH_600 adsorbents were discovered at approximately 8.0 and 10.0, respectively. In terms of adsorption study, the fluoride adsorptions on CNP_600 and CNP_0.2NaOH_600 adsorbents reached the equilibrium stage after 6 h of contact time. Those adsorbents fitted well with the pseudo-2^{nd}-order kinetic model. It was declared that the adsorption process was a chemisorption process. In addition, the isotherm study exhibited the best fit with the Langmuir model and material characteristics properties on CNP_0.2NaOH_600 resulting in mono-layer adsorption combined with ion exchange and electrostatic interaction. Interestingly, the comparative experimental and DFT study on the adsorption mechanism of CNP and F^- ions exhibited the same possible mechanisms which are H-bonding and electrostatic attraction. The absorption of fluoride by using carbonizing biomass waste (Napier grass-derived adsorbent) and modified with alkaline conditions represented a sustainable and innovative solution to mitigate fluoride contamination in groundwater. By converting biomass waste into a valuable adsorbent, communities can achieve safer water sources while simultaneously addressing waste management and environmental conservation goals. Utilizing carbonized biomass waste for fluoride removal offers several advantages: 1) sustainability: Carbonization repurposes biomass waste, contributing to sustainable waste management 2) cost-effectiveness: biomass waste is often abundant and low-cost, making the production of activated carbon economically viable 3) environmental benefits: by utilizing biomass waste, the carbonization process aligns with environmental conservation goals and reduces the reliance on synthetic adsorbents and 4) increased health protection from the high excess F^- concentration in groundwater by using low-cost and sustainable materials.

Acknowledgments

This research work was supported by Chiang Mai University, Thailand. Special thanks are extended to the Department of Environmental Engineering, Faculty of Engineering, Chiang Mai University, Thailand for invaluable support in terms of facilities and scientific equipment. N.Y. thanks the National Research Council of Thailand, Thailand (NRCT): N42A670101 for the computational sources.

References

[1] P Loganathan, S Vigneswaran, J Kandasamy and R Naidu. Defluoridation of drinking water using adsorption processes. *Journal of Hazardous Materials* 2013; **248-249**, 1-19.

[2] M Jiménez-Reyes and M Solache-Ríos. Sorption behavior of fluoride ions from aqueous solutions by hydroxyapatite. *Journal of Hazardous Materials* 2010; **180(1-3)**, 297-302.

[3] A Bhatnagar, E Kumar and M Sillanpää. Fluoride removal from water by adsorption-a review. *Chemical Engineering Journal* 2011; **171(3)**, 811-840.

[4] WHO. *Guidelines for drinking-water quality: Fourth* edition *incorporating the first and second addenda*. World Health Organization, Geneva, Switzerland, 2017.

[5] C Rojanaworarit, L Claudio, N Howteerakul, A Siramahamongkol, P Ngernthong, P Kongtip and S Woskie. Hydrogeogenic fluoride in groundwater and dental fluorosis in Thai agrarian communities: A prevalence survey and case-control study. *BMC Oral Health* 2021; **21(1)**, 545.

[6] N Theerawasttanasiri, S Taneepanichskul, W Pingchai, Y Nimchareon and S Sriwichai. Implementing a geographical information system to assess endemic fluoride areas in Lamphun, Thailand. *Risk Management and Healthcare Policy* 2018; **11**, 15-24.

[7] R Kumar, P Sharma, PK Rose, PK Sahoo, P Bhattacharya, A Pandey and M Kumar. Co-transport and deposition of fluoride using rice

husk-derived biochar in saturated porous media: Effect of solution chemistry and surface properties. *Environmental Technology & Innovation* 2023; **30**, 103056.

[8] KK Shimabuku, ME Baumgardner, RB Bahr, NR Frojelin, AM Kennedy, KT Nolan and NE Stanton. Fluoride removal in batch and column systems using bone char produced in a top-lit updraft drum gasifier and furnace. *Water Research* 2023; **244**, 120332.

[9] NA Tajuddin, EFB Sokeri, NA Kamal and M Dib. Fluoride removal in drinking water using layered double hydroxide materials: Preparation, characterization and the current perspective on IR4.0 technologies. *Journal of Environmental Chemical Engineering*, 2023; **11(3)**, 110305.

[10] MM Damtie, YC Woo, B Kim, RH Hailemariam, KD Park, HK Shon, C Park and JS Choi. Removal of fluoride in membrane-based water and wastewater treatment technologies: Performance review. *Journal of Environmental Management* 2019; **251**, 109524.

[11] J He, Y Yang, Z Wu, C Xie, K Zhang, L Kong and J Liu. Review of fluoride removal from water environment by adsorption. *Journal of Environmental Chemical Engineering* 2020; **8(6)**, 104516.

[12] JL Marco-Brown, M Melotta, M Fernández and A Iriel. Arsenic and fluoride adsorption from multielement solutions onto aluminum-modified montmorillonite. *Groundwater for Sustainable Development* 2024; **26**, 101205.

[13] J Shen and A Schäfer. Removal of fluoride and uranium by nanofiltration and reverse osmosis: A review. *Chemosphere* 2014; **117**, 679-691.

[14] F Aziz, I Din, F Khan, P Manan, A Sher and S Hakim. Treatment of fluoride-contaminated water using mango (Mangifera indica) leaves powder as an adsorbent. *Current Research in Green and Sustainable Chemistry* 2023; **6(25)**, 100359.

[15] R Kumar, P Sharma, W Yang, M Sillanpää, J Shang, P Bhattacharya, M Vithanage and JP Maity. State-of-the-art research progress on adsorptive removal of fluoride-contaminated water using biochar-based materials: Practical feasibility through reusability and column transport studies. *Environmental Research* 2022; **214(4)**, 114043.

[16] Q Wang, Y Li, Z Yu, X Li, S Yin, W Ji, Y Hu, W Cai and X Wang. Highly porous carbon derived from hydrothermal-pyrolysis synergistic carbonization of biomass for enhanced CO_2 capture. *Colloids and Surfaces A: Physicochemical and Engineering Aspects* 2023; **673**, 131787.

[17] AH Jawad, AS Waheeb, RA Rashid, WI Nawawi and E Yousif. Equilibrium isotherms, kinetics, and thermodynamics studies of methylene blue adsorption on pomegranate (*Punica granatum*) peels as a natural low-cost biosorbent. *Desalination and Water Treatment* 2018; **105**, 322-331.

[18] H Shao, Y Li, L Zheng, T Chen and J Liu. Removal of methylene blue by chemically modified defatted brown algae Laminaria japonica. *Journal of the Taiwan Institute of-Chemical Engineers* 2017; **80**, 525-532.

[19] AD Becke. Density-functional exchange-energy approximation with correct asymptotic behavior. *Physical Review A* 1988; **38(6)**, 3098-3100.

[20] S Grimme, J Antony, S Ehrlich and H Krieg. A consistent and accurate ab initio parametrization of density functional dispersion correction (DFT-D) for the 94 elements H-Pu. *The Journal of Chemical Physics* 2010; **132(15)**, 154104.

[21] M Odelius, M Bernasconi and M Parrinello. Two-dimensional ice adsorbed on mica surface. *Physical Review Letters* 1997; **78(14)**, 2855-2858.

[22] SH Vosko, L Wilk and M Nusair. Accurate spin-dependent electron liquid correlation energies for local spin density calculations: A critical analysis[1]. *Canadian Journal of Physics* 1980; **58**, 1-12.

[23] Y Qi, Z Zhou, R Xu, Y Dong, Z Zhang and M Liu. Effect of NaOH pretreatment on permeability and surface properties of three wood species. *ACS Omega* 2023; **8(43)**, 40362-40374.

[24] P Induvesa, R Rattanakom, S Sriboonnak., C Pumas, K Duangjan, P Rakruam, S Nitayavardhana, P Sittisom and A Wongrueng. Adsorption of fluoride onto acid-modified low-cost pyrolusite ore: Adsorption characteristics and efficiencies. *International Journal of*

Environmental Research and Public Health 2022; **19(24)**, 17103.

[25] AK Yadav, AK Chaubey, S Kapoor, T Pratap, B Preetiva, V Vimal and D Mohan. Sustainable Napier grass (*Pennisetum purpureum*) biochar for the Sorptive removal of acid orange 7 (AO7) from water. *Processes* 2024; **12(6)**, 1115.

[26] J Qin, J Wang, J Long, J Huang, S Tang, H Hou and P Peng. Recycling of heavy metals and modification of biochar derived from Napier grass using HNO_3. *Journal of Environmental Management* 2022; **318(62-68)**, 115556.

[27] R Qadeer, J Hanif, M Saleem and M Afzal. Characterization of activated-charcoal. *Journal of the Chemical Society of Pakistan* 1994; **16(4)** 229-235.

[28] A Shaaban, SM Se, NMM Mitan and MF Dimin. Characterization of biochar derived from rubber wood sawdust through slow pyrolysis on surface porosities and functional groups. *Procedia Engineering* 2013; **68**, 365-371.

[29] W Tongpoothorn, M Sriuttha, P Homchan, S Chanthai and C Ruangviriyachai. Preparation of activated carbon derived from *Jatropha curcas* fruit shell by simple thermo-chemical activation and characterization of their physico-chemical properties. *Chemical Engineering Research and Design* 2011; **89(3)**, 335-340.

[30] R Khezri, WAWAK Ghani, DRA Biak, R Yunus and K Silas. Experimental evaluation of Napier grass gasification in an auto thermal bubbling fluidized bed reactor. *Energies* 2019; **12(8)**, 1517.

[31] HVRD Santos, PS Scalize, FJC Teran and RMF Cuba. Fluoride removal from aqueous medium using biochar produced from coffee ground. *Resources* 2023; **12(7)**, 84.

[32] S Guilhen, T Watanabe, T Silva, S Rovani, J Marumo, J Tenório, O Masek and LD Araujo. Role of point of zero charge in the adsorption of cationic textile dye on standard Biochars from aqueous solutions: Selection criteria and performance assessment. *Recent Progress in Materials* 2022; **4(2)**, 1.

[33] Y Ren, M He, G Qu, N Ren, P Ning, Y Yang, X Chen, Z Wang and Y Hu. Study on the mechanism of removing fluoride from wastewater by oxalic acid modified aluminum ash-carbon slag-carbon black doped composite. *Arabian Journal of Chemistry* 2023; **16(5)**, 104668.

[34] DSGD Senewirathna, S Thuraisingam, S Prabagar and J Prabagar. Fluoride removal in drinking water using activated carbon prepared from palmyra (*Borassus flabellifer*) nut shells. *Current Research in Green and Sustainable Chemistry* 2022; **5(6)**, 100304.

[35] NT Hue and TN Hoang. Study about doping ion La^{3+} onto the surface of pyrolusite ore for removing simultaneously both fluoride and phosphate from wastewater. *Journal of Chemistry* 2017; **2017(2)**, 11.

[36] TL Tan, PA Krusnamurthy, H Nakajima and SA Rashid. Adsorptive, kinetics and regeneration studies of fluoride removal from water using zirconium-based metal-organic frameworks. *RSC Advances* 2020; **10(32)**, 18740-18752.

[37] M Yousefi, S Arami, H Takallo, M Hosseini, M Radfarad, H Soleimani and A Mohammadi. Modification of pumice with HCl and NaOH enhancing its fluoride adsorption capacity: Kinetic and isotherm studies. *Human and Ecological Risk Assessment: An International Journal* 2018; **25(6)**, 1-13.

[38] M Regassa, F Melak, W Birke and E Alemayehu. Defluoridation of water using natural and activated coal. *International Advanced Research Journal in Science, Engineering and Technology* 2016; **3(1)**, 1-7.

[39] HVRD Santos, PS Scalize, FJC Teran and RMF Cuba. Fluoride removal from aqueous medium using biochar produced from coffee ground. *Resources* 2023; **12(7)**, 84.

[40] S Bibi, A Farooqi, A Yasmin, MA Kamran and NK Niazi. Arsenic and fluoride removal by potato peel and rice husk (PPRH) ash in aqueous environments. *International Journal of Phytoremediation* 2017; **19(11)**, 1029-1036.

[41] D Mohan, R Sharma, VK Singh, P Steele and CU Pittman. Fluoride removal from water using bio-char, a green waste, low-cost adsorbent: Equilibrium uptake and sorption dynamics modeling. *Industrial & Engineering Chemistry Research* 2012; **51(2)**, 900-914.

[42] Y Wei, L Wang, H Li, W Yan and J Feng. Synergistic fluoride adsorption by composite

adsorbents synthesized from different types of materials-a review. *Frontiers in Chemistry* 2022; **10**, 900660.

[43] J Hoslett, H Ghazal, N Mohamad and H Jouhara. Removal of methylene blue from aqueous solutions by biochar prepared from the pyrolysis of mixed municipal discarded material. *Science of The Total Environment* 2020; **714**, 136832.

[44] H Yu, Y Zhang, L Wang, Y Tuo, S Yan, J Ma, X Zhang, Y Shen, H Guo and L Han. Experimental and DFT insights into the adsorption mechanism of methylene blue by alkali-modified corn straw biochar. *RSC Advances* 2024; **14(3)**, 1854-1865.

[45] Z Zhao, T Nie and W Zhou. Enhanced biochar stabilities and adsorption properties for tetracycline by synthesizing silica-composited biochar. *Environmental Pollution* 2019; **254**, 113015.

[46] B Sawangjang, P Induvesa, A Wongrueng, C Pumas, S Wattanachira, P Rakruam, P Punyapalakul, S Takizawa and E Khan. Evaluation of fluoride adsorption mechanism and capacity of different types of bone char. *International Journal of Environmental Research and Public Health* 2021; **18(13)**, 6878.

[47] A Wongrueng, B Sookwong, P Rakruam and S Wattanachira. Kinetic adsorption of fluoride from an aqueous solution onto a dolomite sorbent. *Engineering Journal* 2016; **20(3)**, 1-9.

[48] N Nabbou, M Belhachemi, M Boumelik, T Merzougui, D Lahcene, Y Harek, AA Zorpas and M Jeguirim. Removal of fluoride from groundwater using natural clay (kaolinite): Optimization of adsorption conditions. *Comptes Rendus Chimie* 2019; **22(2-3)**, 105-112.